Ellipsometric studies of nanocrystalline silicon films with the thicknesses less than 100 nm

Buchenko V. V. and Goloborodko A. A.

Taras Shevchenko National University of Kyiv, 64/13 Volodymyrska Street, Kyiv, 01601, Ukraine, vbu4enko@gmail.com

Received: 09.06.2016

Abstract. Our study deals with the structure of thin nanosilicon films having the thicknesses less than 100 nm. It is measured using multi-angular and spectral ellipsometry methods. Modelling of angular dependences of the ellipsometric parameters shows a significant dependence of both structure and composition of the nanosilicon films upon their thickness. In particular, the volume fraction of voids increases with decreasing thickness of the film. The effect of SiO_x shell of the nanocrystals on the optical properties of our films can be neglected. When the thickness of the nanocrystalline layer is less than 50 nm, the compositions of this layer and the surface-roughness layer become practically identical.

Keywords: nanocrystalline silicon, ellipsometry, polarimetry, chemical vapour deposition, effective medium

PACS: 07.60.Fs, 78.20.-e, 42.25.Gy
UDC: 535.3

1. Introduction

Nanocrystalline silicon, or simply nanosilicon, is widely used in modern integrated electronics [1, 2] and as a promising material for solar cells [3, 4]. It is known that the physical properties of silicon films strongly depend on the conditions of their growth and internal parameters. This has stipulated their comprehensive researches in the recent decades [5–13]. One of the most common methods for growing nanocrystalline silicon films is a chemical vapour deposition [5, 14]. Due to variations of the substrate temperatures and the pressure of a working gas, the structure of deposited films represents a combination of amorphous and crystalline silicon with different ratios of these components [15, 16]. In particular, increasing substrate temperature increases crystallinity of the films [8, 16]. In other words, the conditions of growth of the nanocrystalline silicon films can affect notably their internal structure. On the other hand, the grain size determines the electrical properties of the films, because the grain boundaries are potential barriers for carriers [1, 3]. The recent AFM-studies [10] have demonstrated that the grain size depends on the thickness of deposited films: the films with the thicknesses less than 50 nm contain the grains with the average size 25–30 nm, while the films thicker than 50 nm contain the grains as large as 180–200 nm. This shows that, if the film thickness is less than 100 nm, some reconstruction of its internal structure occurs, thus leading to a sharp change in the nanosilicon grain size. Hence, it is the initial growth stage that determines many physical properties of the nanosilicon films.

Different methods have been used to study thin nanocrystalline silicon films. Among them, spectroscopic ellipsometry represents a high-speed (in fact, real-time) and non-destructive

technique, which is characterized by high enough precision in determining the optical parameters of the films [15–22]. In addition, the spectroscopic ellipsometry allows for determining nanoscale heterogeneity in the transition layers and a surface roughness of the films [16]. According to the AFM [10] and TEM [16] studies, the surface structure depends notably on crystallinity of the film: the greater the latter, the more significant roughness is observed on its surface. Thus, the ellipsometry technique enables one to estimate the internal structure of the nanosilicon films, which is extremely important at the early stages of the film growth.

The present work deals with the studies of optical and structural properties of the thin nanocrystalline silicon films, using the techniques of spectral ellipsometry and multi-angular Mueller polarimetry.

2. Experimental and theoretical backgrounds

Nanocrystalline silicon films were prepared by chemical vapour deposition in a reduced-pressure reactor [10]. Film deposition occurred at the substrate temperature 630°C on crystalline Si substrate covered by a SiO_2 layer with the average thickness 100 nm. The thicknesses of the nanocrystalline films were 85, 50, 10 and 3 nm. Hereafter these films are referred to as samples 1, 2, 3 and 4.

Angular dependences of the ellipsometric parameters were studied with a Muller polarimeter, using the angular set ranging from 10° to 35° (see Ref. [17] for more details). The spectral dependences of the ellipsometric parameters were studied with a rotating-analyzer ellipsometer [6] based on a Beatty method [19]. Here the incident angle of the optical beam was equal to 75° [23–25]. Finally, the resulting errors of the ellipsometric parameters did not exceed 2%.

The interaction of light with the multilayer structure involving M layers is governed by the total reflection coefficient for the *s*- and *p*-polarized components [17]:

$$R^N = r^{0,1} + \sum_{m=1}^{M}\left[\prod_{k=1}^{m}\left(t^{k-1,k}\exp\left(j\frac{2\pi d_k N_k}{\lambda\cos\phi_k}\right)\right)r^{m-1,m}\right], \tag{1}$$

where $r^{i-1,i}$ and $t^{i-1,i}$ denote the amplitude reflection and transmission Fresnel coefficients for the polarizations *s* and *p* of (i–1)-th border [18], d_i and N_i are respectively the thickness and the complex refraction index of *i*-th layer, and ϕ_i is the propagation angle of the light beam in *i*-th layer. In particular, the coefficient $r^{0,1}$ corresponds to the reflectivity between ambient and top layers of the structure.

Eq. (1) evidences that the overall reflection contains the phase factor of each intermediate layer, $\beta_k = 2\pi d_k N_k / (\lambda\cos\phi_k)$, which represents phase incursion during the wave propagation in the layer. This assumes a possibility for interference phenomena appearing as oscillations observed in the angular dependence of the reflectance. Then each set of the angular dependences defines the type of the structure and, therefore, the shape of the corresponding curve allows for determining the composition of the multilayer structure. Analytical expressions available for the angular dependence of the ellipsometric parameters of reflected light and numerical methods used for their solving enable one to restore the unknown characteristics of the medium, the thickness of layers and their complex refractive indices. However, extraction of the impact of each layer of the structure on the reflected radiation is non-trivial. This problem relies upon solving the system of transcendent Eqs. (1) with the set of arguments:

$$\frac{R_{pi}}{R_{si}} = \tan\psi_i \exp(j\Delta_i) = \frac{r_p(\{N\},\{d\})}{r_s(\{N\},\{d\})}, \tag{2}$$

where i is the number of equations, and $\{N\}$ and $\{d\}$ are the sets of refractive indices and thicknesses of the layers of the structure, respectively. To simplify the problem, one can employ an effective medium model [15], which facilitates getting the solution. Note that the studies of angular dependence of the ellipsometric parameter enable one to obtain a required number of independent equations for determining the optical parameters of the structure. The final solution of the problem is such sets of the thicknesses of the layers and their complex refractive indices, which reduce to minimum the standard deviation of the experimental and theoretical data,

$$\sigma = \sqrt{\frac{1}{2M-P-1}\sum_{i=1}^{N}\left(\left(\psi_i^{calc}-\psi_i^{meas}\right)^2+\left(\Delta_i^{calc}-\Delta_i^{meas}\right)^2\right)}. \tag{3}$$

Here M is the number of measured pairs of the ellipsometric parameters ψ and Δ, P the number of unknown parameters, and symbols '*meas*' and '*calc*' indicate respectively measured and calculated parameter values.

3. Results and discussion

Fig. 1 displays the angular dependences of the ellipsometric parameters of reflected light, as measured for all of our samples. Here full and open circles refer to the experimental data. The samples have been studied at the helium-neon laser wavelength (λ = 633 nm), and all the results have been averaged over six points. Solid and dashed curves appearing in Fig. 1 correspond to the calculated angular dependences of the ellipsometric parameters. A four-layer model has been employed to simulate the optical parameters of the films, as illustrated in Fig. 2. It is worthwhile to notice that a complex (e.g., non-spherical) shape of the grains forming the film can have its manifestations in the polarization parameters of reflected light studied at the incident angles 20–40^o [17, 26].

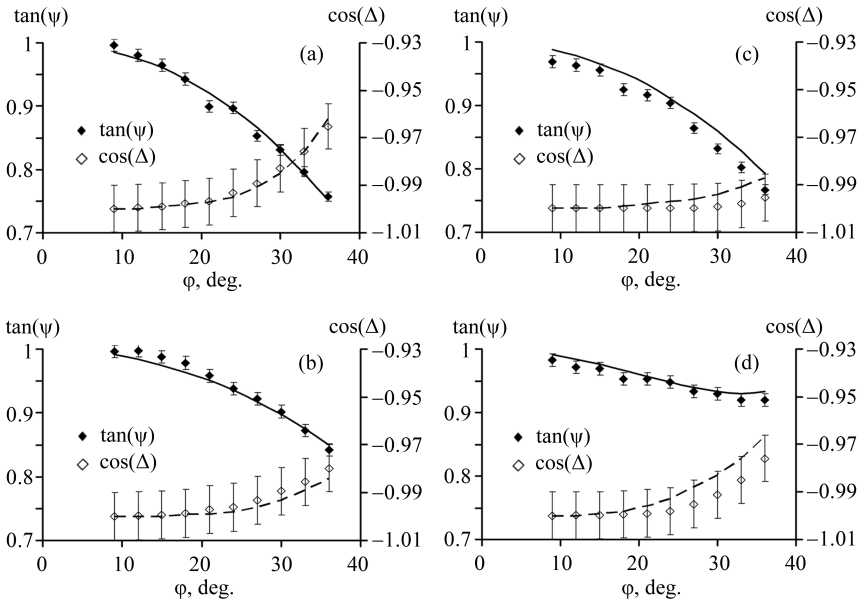

Fig. 1. Angular dependences of ellipsometric parameters obtained for the samples 1 (a), 2 (b), 3 (c) and 4 (d). Full and open circles correspond to experimental angular dependences of tanψ and cosΔ, respectively. Solid and dashed curves label simulated angular dependences of tanψ and cosΔ, respectively. The model parameters are gathered in Table 1.

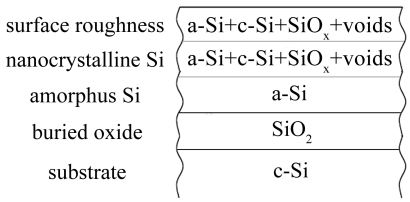

Fig. 2. Optical model of our samples.

When modelling the ellipsometric parameters, we have used a Bruggeman effective-medium approximation [15]. In this study, the dielectric function of nc-Si is described by a mixture of crystalline silicon (c-Si), amorphous silicon (a-Si), SiO_2 and voids [20–22]. The optical constants n and k for these substances at 633 nm are as follows: $n_{\text{c-Si}} = 3.87$, $k_{\text{c-Si}} = 0.001$, $n_{\text{a-Si}} = 4.21$, $k_{\text{a-Si}} = 0.422$, and $n_{\text{SiO2}} = 1.45$ [27, 28]. We have treated the volume fractions of these components as model parameters in the theoretical calculations of the ellipsometric parameters. The standard deviation between the experimental and theoretical data does not exceed 5% for all of our samples. As seen from Fig. 1 a, b, the simulation reproduces the best the experimental data obtained for the samples 1 and 2. At the same time, the coincidence of the experimental and simulation data is slightly worse for the samples 3 and 4 (see Fig. 1c, d).

Table 1. Model parameters of the effective medium: a-Si is amorphous silicon.

Layer / Sample	a-Si	Nanocrystalline layer (nc-Si)				Surface-roughness layer [15]			
	d, nm	d, nm	Volume fraction			d, nm	Volume fraction		
			c-Si	a-Si	voids		c-Si	a-Si	voids
1	0	85	0.61	0.38	0.01	12	0.66	0.01	0.33
2	0	50	0.81	0.04	0.15	2	0.8	0.01	0.19
3	8	4	0.55	0.08	0.37	5	0.4	0.03	0.57
4	0	4	0.33	0.05	0.62	1	0.28	0.07	0.65

Using the simulations of the angular dependences of the ellipsometric parameters, we have obtained the parameters of the effective medium shown in Table 1. Although Si clusters can, in principle, easily react with residual O_2 in the chamber, the data presented in Table 1 confirm that the effect of SiO_x shells surrounding Si clusters on the parameters of the films could be neglected. According to Ref. [29], both porous and macrocrystalline silicon films should be considered as silicon clusters with SiO_x shells. In Ref. [10] it has been assumed that the corresponding grains grow basing on crystal lattice rotation, and so the film growth is accompanied by formation of stress defects (e.g., cracks of the crystal lattice). Moreover, silicon oxide clusters are not formed due to a high temperature of the substrate [30]. As a result, we assume that the Mueller polarimetric data confirm the above assumptions about the grain growth.

As seen from Table 1, the effective-medium parameters found for the sample 3 are quite different from those of the samples 1, 2 and 4. In this relation we mention that our films have been prepared at a high enough temperature, 630°C [10]. According to Ref. [31], thin nanocrystalline silicon films have a uniform fine-grained structure, with the average grain size of 20 nm. At the same time, the effect of diffusion phenomena on the structure of the films can be strong due to high temperatures. Then the films with the thickness 5 nm have insular character, with general border junctions [31]. Aggregation of the grains in agglomerates occurs with increasing film thick-

ness up to 10 nm, which is accompanied by changing grain borders, which are now featured by the presence of triple joints [31, 32]. It has also been assumed that the cumulative effect of grain growth associated with crystal lattice rotation, on the one hand, and high-temperature conditions, on the other hand, can lead to the formation of amorphous films [10]. At the same time, further sputtering of silicon at 630°C can result in the formation of tension defects, which is accompanied by formation of fibrous nanosilicon films and disappearance of the amorphous phase [3].

One can observe a significant contribution of amorphous silicon to the dielectric function of the nanocrystalline layer in case of sample 1, which has a sharply reduced layer of surface roughness. This may be owing to large dispersion in the grain-size distribution for the films having the thicknesses less than 50 nm [10]. Then we observe a large volume fraction of the crystalline silicon in the nanocrystalline layer and the surface-roughness layer. The contribution of voids into the dielectric function of the nanocrystalline layer increases significantly for the samples 3 and 4, whereas the contribution of the amorphous silicon becomes negligible. It is worth to emphasize that a satisfactory agreement between the experimental curves and the simulation data for the samples 1, 2 and 4 can be obtained with a zero thickness of the amorphous silicon layer. As seen from Table 1, the volume fractions of the components obtained for the nanocrystalline layer and the surface-roughness layer are almost indistinguishable for those samples. Of course, decreasing layer thickness reduces the accuracy of determination of its optical constants. Moreover, the changes in the optical constants of a layer have a negligible effect on the ellipsometric parameters of the reflected light provided that the layer thickness decreases.

To calculate the spectral dependences of the ellipsometric parameters, we have used the Bruggeman model. Then the data collected in Table 1 have been taken as the model parameters of the structure. The spectral dependences of the ellipsometric parameters of our samples are shown in Fig. 3.

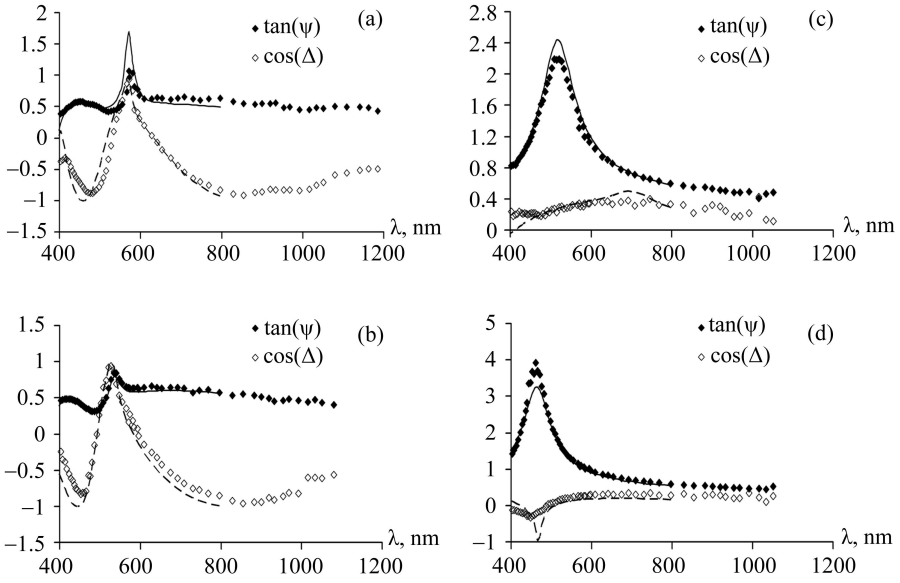

Fig. 3. Spectral dependences of ellipsometric parameters obtained for the samples 1 (a), 2 (b), 3 (c) and 4 (d). Full and open circles correspond to experimental spectral dependences of tanψ and cosΔ, respectively. Solid and dashed curves label the simulated spectral dependences of tanψ and cosΔ, respectively. The model parameters are gathered in Table 1.

As seen from Fig. 3, the spectral curves obtained for the samples 1 and 2, 3 and 4 are very similar. In general, the character of spectral dependences of the ellipsometric parameters indicates restructuring of the nanocrystalline films that occurs with increasing film thickness. In case of the samples 1 and 2, the thickness of the film shifts significantly the phase of reflected radiation, while the samples 3 and 4 with thinner nanocrystalline layers have a small effect on the phase shift between the *s*- and *p*-polarizations of reflected light. Thus, the spectral curves of the ellipsometric parameters obtained for the samples 3 and 4 appear to be similar to those typical for the clean-silicon surface [15]. Our final note concerns a discrepancy between the calculated and experimental spectral dependences of the ellipsometric parameters. It is caused by the changes in the electron-band structure of the film composed of nanoscale grains, when compared with the structure of crystalline silicon [33–35].

4. Conclusion

The analysis of angular dependences of the ellipsometric parameters of our nanocrystalline silicon film samples has revealed a strong correlation of the physical properties and the internal structure of our samples with the thickness of the nanocrystalline layer. When this thickness decreases from 85 down to 50 nm, one can observe a significant increase in the volume fractions of voids available in the nanocrystalline layer. Moreover, the properties of the latter layer and the surface-roughness layer become almost identical whenever the samples with the film thicknesses as small as 3 nm and 10 nm are dealt with. Our modelling has also demonstrated that the influence of SiO_x layers located around Si clusters can be neglected and the dielectric function of the nanocrystalline silicon layer is similar to that of the crystalline silicon. However, in case of the sample with the layer thickness of 10 nm, the simulated angular and spectral dependences of the ellipsometric parameters correlate with the relevant experimental data only after taking into account a thin amorphous-silicon layer between the nanocrystalline silicon film and the SiO_2 layer.

Acknowledgements

The authors are grateful to Dr. Kolomiets I. S. for his help with polarimetric measurements, and to Dr. Kovalenko A. V. for critical reading of the manuscript and useful comments.

References

1. Nakhodkin N, Kulish N and Rodionova T, 2010. Faceting of twin grain boundaries in polysilicon films. Phys. Status Solidi (a) **207**: 316–320.
2. Spott A, Peters J, Davenport M L, Stanton E J, Merritt C D, Bewley W W, Vurgaftman I, Kim C S, Meyer J. R, Kirch J, Mawst L J, Botez D and Bowers J E, 2016. Quantum cascade laser on silicon. Optica **3**: 45–551.
3. Nakhodkin N G, Kulish N P and Rodionova T V, 2013. Faceting of twin tips in polysilicon films. J. Cryst. Growth. **381**: 65–69.
4. Rath J K, 2003. Low temperature polycrystalline silicon: a review on deposition, physical properties and solar cell applications. Solar Energy Mater. and Solar Cells. **76**: 431–487.
5. Dana S S, Anderle M, Rubloff GW and Acovic A, 1993. Chemical vapor deposition of rough-morphology silicon films over a broad temperature range. Appl. Phys. Lett. **63**: 1387–1389.
6. Goloborodko A A, Epov M V, Robur L Y and Rodionova TV, 2014. Multiangular and spectral ellipsometry for semiconductor nanostructures classification. J. Nano-Electron. Phys. **6**: 02002(1–5).
7. Ishihara S, He D and Shimizu I, 1994. Structure of polycrystalline silicon thin film fabricated

from fluorinated precursors by layer-by-layer technique. Japan. J. Appl. Phys. **33**: 51–56.
8. Murata K, Ito M, Hori M and Goto T, 1999. Control of seed layer for a low temperature formation of polycrystalline silicon with high crystallinity and a smooth surface. J. Vac. Sci. Technol. **17**: 1098–1100.
9. Mukhopadhyay S, Chowdhury A and Ray S, 2008. Nanocrystalline silicon: A material for thin film solar cells with better stability. Thin Solid Films. **516**: 6824–6828.
10. Nakhodkin N, Rodionova T and Sutyagina A, 2015. Mechanisms of surface evolution during the growth of undoped nanosilicon films. Ukr. Journ. Phys. **60**: 166–170.
11. Shin J H and Huh H, 2000. Direct low-temperature chemical vapor deposition of fully crystalline micro- and polycrystalline silicon thin films on SiO_2 using plasma immersion ion implantation. J. Vac. Sci. Technol. A. **18**: 51–57.
12. Mirgorodskiy IV, Golovan L A, Timoshenko V Y, Semenov A V and Puzikov V M, 2014. Luminescence properties of thin nanocrystalline silicon-carbide films fabricated by direct-beam ion deposition. Semiconductors. **48**: 711–714.
13. Mussabek G, Mirgorodskij I, Kharin A, Taurbayev T and Timoshenko V, 2015. Formation and optical properties of nanocomposite based on silicon nanocrystals in polymer matrix for solar cell coating. J. Nanoelectron. Optoelectron. **9**: 738–740.
14. Becker C, Amkreutz D, Sontheimer T, Preidel V, Lockau D and Haschke J, 2013. Polycrystalline silicon thin-film solar cells: Status and perspectives. Solar Energy Mater. and Solar Cells. **119**: 112–123.
15. Petrik P, Lohner T, Fried M, Biro L, Khanh N, Gyulai J, Lehnert W, Schneider C and Ryssel H, 2000. Ellipsometric study of polycrystalline silicon films prepared by low-pressure chemical vapor deposition. J. Appl. Phys. **87**: 1734–1742.
16. Borghesi A, Giardini M E, Marazzi M, Sassella A and Santi G D, 1997. Ellipsometric characterization of amorphous and polycrystalline silicon films deposited using a single wafer reactor. Appl. Phys. Lett. **70**: 892–894.
17. Barchuk O I, Bilenko K S, Goloborodko A A, Kurashov V N, Oberemok E A and Savenkov S N., 2009. Influence of structure of polysilicon films on optical characteristics of the reflected light. Nanosystems, Nanomaterials, Nanotechnology. **7**: 421–431.
18. Fujiwara H, Spectroscopic ellipsometry: principles and applications. Chichester: John Wiley & ons Ltd, 2007.
19. Tompkins H G, A users's guide to ellipsometry. London: Academic Press Inc., 1993.
20. Vuye G, Fisson S, Van Nguyen V, Wang Y, Rivory J and Abeles F, 1993. Temperature dependence of the dielectric function of silicon using in situ spectroscopic ellipsometry. Thin Solid Films. **233**: 166–170.
21. Pierce D T and Spicer W E, 1972. Electronic structure of amorphous Si from photoemission and optical studies. Phys. Rev. B. **5**: 3017–3029.
22. Malitson I H, 1965. Interspecimen comparison of the refractive index of fused silica. J. Opt. Soc. Amer. **55**: 1205–1208.
23. Kostruba A, Stetsyshyn Yu and Vlokh R, 2015. Method for determination of the parameters of transparent ultrathin films deposited on transparent substrates under conditions of low optical contrast. Appl. Opt. **54**: 6208–6216.
24. Colard S, 1999. Optimisation of experimental conditions for variable angle spectroscopic ellipsometry analysis. Application to GaAs/(Al,Ga)As quantum well characterisation. Mater. Sci. Eng. B. **66**: 88–91.

25. Kostruba A M, 2003. Optimization of experimental conditions for ellipsometric studies of ultra-thin absorptive films. Ukr. J. Phys. Opt. **4**: 177–186.
26. Kolomiets IS, Savenkov SN and Oberemok YeA, 2015. Polarization properties of longitudinally inhomogeneous dichroic medium. Semiconductor Physics, Quant. Electron. & Optoelectron. **18**: 193–199.
27. Palik E D, Handbook of optical constants of solids. Burlington: Academic Press, 2002.
28. Sobolev V.V., Sobolev VVal and Shushkov SV, 2011. Optical spectra of the six phases of the silicon, Semiconductors **45**: 1247–1250.
29. Golovan L A, Timoshenko V Yu and Kashkarov P K, 2007. Optical properties of porous-system-based nanocomposites. Sov. Phys. Uspekhi. **50**: 595–612.
30. Nakhodkin NG, Kulish NP and Rodionova TV, 2003. Orientation relationships in dendritic polysilicon films. J. Surf. Investig.: X-Ray, Synchrotron and Neutron Techniques. **19**: 17–20.
31. Nakhodkin NG, Kulish NP, Lytvyn P M, Rodionova TV and Sutyigina A, 2012. Effect of thickness on structural characteristics of nanosilicon films. Bulletin of Taras Shevchenko National University of Kyiv, Series 'Physics & Mathematics'. **1**: 285–288.
32. Nakhodkin NG, Kulish NP, Lytvyn PM and Rodionova TV, 2006. Features of special joints of grain boundaries in polysilicon films of equiaxial and dendritic structures. Functional Mater. **2**: 305–309.
33. Wang X X, Zhang J G, Ding L, Cheng B W, Ge W K, Yu J Z and Wang Q M, 2005. Origin and evolution of photoluminescence from Si nanocrystals embedded in a SiO_2 matrix. Phys. Rev. B. **72**: 195313.
34. Creekmore S, Seo J T, Yang Q, Wang Q, Anderson J, Pompey C and Temple D, 2003. Nonlinear optical properties of cadmium telluride semiconductor nanocrystals for optical power-limiting application. J. Korean Phys. Soc. **42**: S143–S148.
35. Kravets V, 2013. Silicon nanoparticles: their photoluminescence, complex refractive index, and relationship with the band structure. Opt. Spectrosc. **114**: 230–235.

Buchenko V. V. and Goloborodko A. A. 2016. Ellipsometric studies of nanocrystalline silicon films with the thicknesses less than 100 nm. Ukr.J.Phys.Opt. **17**: 124 – 131

Анотація. *Стаття присвячена вивченню структури тонких нанокремнійових плівок з товщинами, меншими 100 нм, за методами багатокутової та спектральної еліпсометрії. Моделювання кутових залежностей еліпсометричних параметрів показало істотну залежність структури і складу нанокремнійових плівок від їхньої товщини. Зокрема, зі зменшенням товщини плівки зростає об'ємна частка пустот. Доведено, що впливом нанокристалічної оболонки SiO_x на оптичні властивості плівок можна знехтувати. Нарешті, за товщини нанокристалічного шару, меншої 50 нм, склад цього шару і шару поверхневої шорсткості практично однаковий.*